**Annales
Geophysicae**

Non-storm irregular variation of the D_{st} index

S. Nakano and T. Higuchi

The Institute of Statistical Mathematics, Tachikawa, Japan

Correspondence to: S. Nakano (shiny@ism.ac.jp)

Abstract. The D_{st} index has a long-term variation that is not associated with magnetic storms. We estimated the long-term non-storm component of the D_{st} variation by removing the short-term variation related to magnetic storms. The results indicate that the variation of the non-storm component includes not only a seasonal variation but also an irregular variation. The irregular long-term variation is likely to be due to an anti-correlation with the long-term variation of solar-wind activity. In particular, a clear anti-correlation is observed between the non-storm component of D_{st} and the long-term variation of the solar-wind dynamic pressure. This means that in the long term, the D_{st} index tends to increase when the solar-wind dynamic pressure decreases. We interpret this anti-correlation as an indication that the long-term non-storm variation of D_{st} is influenced by the tail current variation. The long-term variation of the solar-wind dynamic pressure controls the plasma sheet thermal pressure, and the change of the plasma sheet thermal pressure would cause the non-storm tail current variation, resulting in the non-storm variation of D_{st}.

Keywords. Geomagnetism and paleomagnetism (Time variations, diurnal to secular) – Magnetospheric physics (General or miscellaneous)

1 Introduction

The D_{st} index exhibits long-term variations with time scales longer than the duration of a magnetic storm (e.g. Mayaud, 1978). These long-term variations are related primarily to the long-term variations of magnetic storm activity. For example, the semi-annual variation of magnetic storm activity is an important part of the long-term variation of the D_{st} index (e.g. Cliver et al., 2000; O'Brien and McPherron, 2002). On the other hand, the D_{st} index also has a non-storm long-term variation. Figure 1 indicates the daily means of the D_{st} index

for eight years from 1996 to 2003. Negative spikes correspond to magnetic storms, and positive spikes are attributed to the enhancement of the magnetopause current caused by the enhancement of the solar-wind dynamic pressure. If we ignore such spikes, we can make out a long-term variation that is not associated with magnetic storms. This non-storm long-term variation appears to be roughly periodic. In fact, the quiet-time D_{st} index exhibits seasonal variations (Cliver et al., 2001; Mursula and Karinen, 2005). However, it does not seem that this periodic variation explains all the features of the non-storm long-term variation, which implies that the non-storm variation also includes some non-periodic irregular variation. This paper focuses on this irregular non-storm variation of the D_{st} index.

Recently, we have devised a method by which to estimate the long-term non-storm component of the D_{st} variation (Nakano and Higuchi, 2009). This method assumes that the short-term variations of the D_{st} index due to magnetic storms can be described by the empirical model by Burton et al. (1975). The non-storm long-term component is then estimated as a component that cannot be explained by this empirical model. In the present report, we analyze the non-storm long-term component estimated using this method. We then describe the characteristics of the non-storm variation of the D_{st} index, especially focusing on the irregular variation.

2 Model for variation of the D_{st} index

Burton et al. (1975) used the following approach to model the temporal variation of the D_{st} index. First, the effect from the magnetopause current is eliminated from D_{st}:

$$D_{st}^* = D_{st} - b\sqrt{P_d} + c, \tag{1}$$

where D_{st}^* represents the pure magnetic-storm disturbance due to the ring current and the tail current, and P_d denotes the dynamic pressure of the solar wind. The temporal evolution
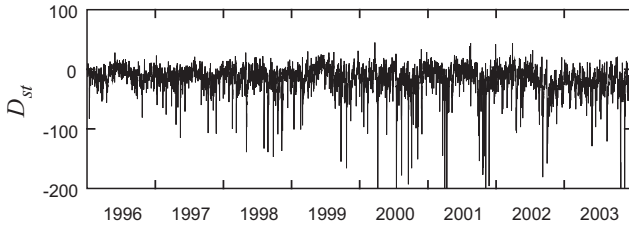
Fig. 1. Time series of daily values of the D_{st} index from 1996 to 2003.

of the pure magnetic-storm effect D_{st}^* can then be modeled as follows:

$$\frac{\Delta D_{st}^*}{\Delta t} = Q - \frac{D_{st}^*}{\tau}. \tag{2}$$

Based on the study by Burton et al., the values of the parameters in Eqs. (1) and (2) have been revised in several studies (e.g. O'Brien and McPherron, 2000; Wang et al., 2003; Xie et al., 2008). For example, according to Xie et al. (2008), the parameters b and c in Eq. (1) are given as:

$$b[\text{nT/nPa}^{1/2}] = 4.2 + 3.5 \exp[-\mathcal{R}(E)] \tag{3}$$

$$c[\text{nT}] = 10.8, \tag{4}$$

where E denotes the solar-wind electric field, and $\mathcal{R}$ is the Ramp function given as

$$\mathcal{R}(x) = \begin{cases} x & \text{if } x \geq 0 \\ 0 & \text{otherwise.} \end{cases} \tag{5}$$

The solar-wind electric field E is given as $E = vB_s$, where v is the solar-wind speed, and B_s is the southward component of the solar-wind magnetic field in the geocentric solar magnetospheric (GSM) coordinate system. The parameter Q, which represents the evolution of D_{st}^*, can be given as follows:

$$Q[\text{nT/h}] = -4.4 (P_d/3)^{0.5} \cdot \mathcal{R}(E - 0.49). \tag{6}$$

Finally, τ is given as follows:

$$\tau[\text{hours}] = \begin{cases} 2.4 \exp[9.74/(4.69 + E)] & \text{if } E > 0 \\ 8.7 \exp[6.66/(6.04 + P_d)] & \text{otherwise.} \end{cases} \tag{7}$$

(We take the equation for τ from the paper by Wang et al. (2003). Xie et al. (2008) gave τ for the case $E \leq 0$ as $-8.7 \exp[6.66/(6.04 + P_d)]$. However, τ must take a positive value, and thus the equation provided by Wang et al. would be correct.)

In principle, once the value of the D_{st} index at a certain time is given, we can thereafter sequentially predict the evolution of D_{st} using Burton's model given by Eqs. (1) and (2) as long as the solar-wind data for P_d, v, and B_s are available.

In general, however, the prediction using the model often deviates from the actual values. We assume that the deviation is due to the long-term non-storm variation and estimate it as a component that cannot be represented by Burton's model. A method for estimating the long-term component is described in the next section.

3　Method of analysis

3.1　Modeling of D_{st} variation

We have previously introduced a method by which to estimate the long-term component of the D_{st} variation, which is based on the parameters given by O'Brien and McPherron (2000) (Nakano and Higuchi, 2009). In the present study, we use a revised method based on the parameters reported by Xie et al. (2008). We decompose the variation of D_{st} into three components as

$$D_{st}^t = D_{RC}^t + D_{MPC}^t + D_{base}^t \tag{8}$$

where D_{st}^t denotes a model D_{st} value at time t, D_{RC}^t denotes the ring-current (and tail-current) effect on D_{st}, D_{MPC}^t denotes the magnetopause-current effect, and D_{base}^t denotes a non-storm long-term component that is related to neither the storm-time ring-current nor the magnetopause current. The ring-current effect D_{RC} corresponds to D_{st}^* in Eq. (2). The magnetopause-current effect D_{MPC} corresponds to the term $b\sqrt{P_d}$ in Eq. (1). The non-storm component D_{base} corresponds to the term c in Eq. (1), which gives the base level of the D_{st} when both D_{RC} and D_{MPC} are zero.

Here, we model a transition of a state of D_{RC}^t for each hour ($\Delta t = 1$[hour]) on the basis of Eq. (2), as follows:

$$D_{RC}^t = D_{RC}^{t-1} - 4.4 \left(\frac{P_d^{t-1}}{3}\right)^{0.5} \cdot \mathcal{R}(E^{t-1} - 0.49) - \frac{D_{RC}^{t-1}}{\tau^t}, \tag{9}$$

where E^{t-1} and P_d^{t-1} denote the solar-wind electric field and the solar-wind dynamic pressure, respectively, at time $t-1$. The decay time τ^t is given as

$$\tau^t = \begin{cases} 2.4 \exp[9.74/(4.69 + E^{t-1})] & \text{if } E^{t-1} > 0 \\ 8.7 \exp[6.66/(6.04 + P_d^{t-1})] & \text{otherwise.} \end{cases} \tag{10}$$

The magnetopause-current effect D_{MPC}^t is described as

$$D_{MPC}^t = b^t \sqrt{P_d^t}, \tag{11}$$

where the coefficient b^t is given according to Eq. (3) as

$$b^t = 4.2 + 3.5 \exp[-\mathcal{R}(E^t)]. \tag{12}$$

The non-storm component D_{base}^t corresponds to $-c$ if written in the manner shown in Eq. (1). In the original study by Burton et al. and in subsequent studies, the base level

of D_{st}, D_{base}, was assumed to be constant independently of time t. On the other hand, we allow a gradual variation of D_{base}. The transition of D_{base}^t is described using a probability density function (PDF), more specifically, a conditional PDF given the previous value D_{base}^{t-1}. We assume that D_{base}^t obeys a normal distribution, in which the mean is the value at the previous time D_{base}^{t-1} and the variance is 0.0025, as follows:

$$p(D_{base}^t | D_{base}^{t-1}) = N(D_{base}^{t-1}, 0.0025), \tag{13}$$

where $p(a|b)$ denotes the conditional PDF of a given b and $N(\mu, \sigma^2)$ denotes the normal distribution with mean μ and variance σ^2. The assumption implies that D_{base}^t is assumed to be very similar but not necessarily equal to the previous state D_{base}^{t-1}. The variance is taken to be as small as 0.0025, which allows the gradual variation of about 0.05 nT per hour in D_{base}. We choose this variance value such that the effects of the variations with time scales shorter than one month will not appear in the auto-correlation function of the estimated D_{base}^t.

3.2 Modeling of solar-wind variation

The model of D_{RC}^t in Eq. (9) requires the solar-wind electric field at the previous time step E^{t-1} as an input. Since the solar-wind electric field can be derived from solar-wind data, which are ordinarily observed by spacecraft, we can predict the value of D_{RC} at the next time step using Eq. (9). However, this prediction would inevitably contain an error because of the following reasons. First, the solar-wind data would contain observation errors. Second, since the coupling between the solar wind and the magnetosphere would be variable, the solar-wind condition should not always agree with the effective electric field contributing to the development of the ring current, even if we can accurately observe the solar-wind conditions.

In order to avoid the influence of the prediction errors, the solar-wind electric field E^t is treated as an uncertain variable. We allow a difference in the electric field between the estimate in the model and the observation, although the electric field in the model is assumed to be similar to the observation, as explained later. We represent a state transition of E^t using a Cauchy distribution with a location parameter of E^{t-1} and a scale parameter of 1 as

$$p(E^t | E^{t-1}) = Cauchy(E^{t-1}, 1). \tag{14}$$

The Cauchy distribution (e.g. Kitagawa, 1996) is used in order to allow large jumps due to discontinuous structure in the solar wind. We also treat the solar-wind dynamic pressure P_d^t, which is used in Eq. (11), as an uncertain variable in order to allow the difference between the magnetopause-current effect inferred from the solar-wind data and the real magnetopause-current effect. Since the solar-wind dynamic pressure P_d^t can not be less than zero, a state transition of P_d^t

is defined using the logarithm of P_d^t as

$$p(\log P_d^t | \log P_d^{t-1}) = N(\log P_d^{t-1}, 1). \tag{15}$$

3.3 Modeling of observation

As described above, we consider a model of the system that consists of seven variables: three components contributing to the D_{st} index, D_{RC}^t, D_{MPC}^t, and D_{base}^t; two solar-wind parameters, P_d^t and E^t; and two auxiliary parameters, τ^t and b^t. However, τ^t is uniquely determined if P_d^{t-1} and E^{t-1} are given according to Eq. (10), b^t is uniquely determined if E^t is given according to Eqs. (12), and D_{MPC}^t is uniquely determined if P_d^t and b^t are given according to Eq. (11). Hence, it is sufficient to consider only four variables (D_{RC}^t, D_{base}^t, P_d^t, and E^t) in order to describe a state transition of this system. We want to estimate the temporal evolution of the four variables in this system model using available observations. From the system, we can use the observations for three variables: D_{st}, P_d, and E. We therefore consider the relationship between the observed value and the model value for each of the three variables.

From the variables considered in the present model, we can obtain a model D_{st} value according to Eq. (8). We can thus describe the relationship between the observed D_{st} data and the model D_{st} value as

$$p(D_{st,obs}^t | D_{st}^t) = N(D_{st}^t, 25) \tag{16}$$

where $D_{st,obs}^t$ denotes the observed D_{st} index. This equation indicates that the observed value $D_{st,obs}^t$ is equal to the model value D_{st}^t on average, but that some difference between the observed value and the model value is allowed. Using Eq. (8), Eq. (16) can be rewritten in the form of the conditional PDF given D_{RC}^t, D_{MPC}^t, and D_{base}^t as

$$\begin{aligned} p(D_{st,obs}^t | D_{RC}^t, \; D_{MPC}^t, \; D_{base}^t) \\ = N(D_{RC}^t + D_{MPC}^t + D_{base}^t, 25) \end{aligned} \tag{17}$$

With respect to the solar-wind parameters P_d and E, the relationships between the observed values and the model values are described as

$$p(P_{d,obs}^t | P_d^t) = N(P_d^t, 1) \tag{18}$$
$$p(E_{obs}^t | E^t) = N(E^t, 1), \tag{19}$$

where $P_{d,obs}^t$ and E_{obs}^t denote the observations of P_d and E, respectively, where P_d^t and E^t denote the values in the model. Thus, P_d and E in the model are assumed to be similar to the observation, although we allow differences between the model and the observation as described above.

In the present paper, we use the data of the D_{st} index provided by the Data Analysis Center for Geomagnetism and Space Magnetism, Kyoto University (http://wdc.kugi.kyoto-u.ac.jp/). For the solar-wind conditions $P_{d,obs}^t$ and

E^t_{obs}, we refer to the OMNI2 solar-wind hourly data provided through the OMNIWeb database of the National Space Science Data Center, NASA (http://omniweb.gsfc.nasa.gov/). Although the original OMNI2 data do not contain the data for the electric field E^t_{obs}, we generate electric field data from the data of the solar-wind speed v^t_{obs} and the southward component of the solar-wind magnetic field in GSM coordinates $B^t_{s,obs}$ as $E_{obs} = v^t_{obs}B^t_{s,obs}$.

3.4 Estimation

For convenience in explaining the estimation method, we assemble the four variables describing the state of the system into a state vector $\boldsymbol{x}_t$ as follows:

$$\boldsymbol{x}_t = \begin{pmatrix} D^t_{RC} \\ D^t_{base} \\ P^t_d \\ E^t \end{pmatrix}. \qquad (20)$$

We now consider a transition of a state $\boldsymbol{x}_t$ by a conditional distribution given the previous state $\boldsymbol{x}_{t-1}$, as $p(\boldsymbol{x}_t|\boldsymbol{x}_{t-1})$, which can be defined by combining conditional PDFs for each component in Eqs. (9), (13), (14), and (15). Although D^t_{RC} is uniquely determined according to Eq. (9) if $\boldsymbol{x}_{t-1}$ is given, the PDF of D^t_{RC} can be represented by a Dirac delta function as

$p(D^t_{RC}|\boldsymbol{x}_{t-1})$

$$= \delta\left(D^t_{RC} - D^{t-1}_{RC} + 4.4\mathcal{R}(E^{t-1} - 0.49) + \frac{D^{t-1}_{RC}}{\tau^t}\right). \qquad (21)$$

We also define an observation vector $\boldsymbol{y}_t$ as

$$\boldsymbol{y}_t = \begin{pmatrix} D^t_{st,obs} \\ P^t_{d,obs} \\ E^t_{obs} \end{pmatrix}. \qquad (22)$$

The relationship between $\boldsymbol{y}_t$ and $\boldsymbol{x}_t$ can be described by a conditional PDF as $p(\boldsymbol{y}_t|\boldsymbol{x}_t)$ which can be defined by combining Eqs. (17) through (19). Although the data of D_{st} are always available, the solar-wind data are sometimes missing. In such situations, we redefine $p(\boldsymbol{y}_t|\boldsymbol{x}_t)$ using only Eq. (17) and refer to only the D_{st} data. The state variables including the solar-wind parameters can be estimated using the solar-wind conditions at the previous time step and the D_{st} variation. However, if the solar-wind data are missing for a long time, the accuracy of the estimate of the state becomes poor. Therefore, we exclude periods during which the solar-wind data are missing for more than 6 h from the analysis.

Thus, $\boldsymbol{x}_t$ must be estimated at each time step using a sequence of observations $\{\boldsymbol{y}_1, \ldots, \boldsymbol{y}_T\}$. Since the PDFs $p(\boldsymbol{x}_t|\boldsymbol{x}_{t-1})$ and $p(\boldsymbol{y}_t|\boldsymbol{x}_t)$ are given for each time step, we can estimate $\boldsymbol{x}_t$ at each time step via Bayesian inference as follows. Suppose that a conditional PDF $p(\boldsymbol{x}_{t-1}|\boldsymbol{y}_{1:t-1})$, which is a posterior distribution given the observations until time

$t-1$ ($\boldsymbol{y}_{1:t-1}$ denotes a sequence of observations from the initial observation time 1 to time $t-1$, $\{\boldsymbol{y}_1, \ldots, \boldsymbol{y}_{t-1}\}$), a predictive distribution at time t is obtained as

$$p(\boldsymbol{x}_t|\boldsymbol{y}_{1:t-1}) = \int p(\boldsymbol{x}_t|\boldsymbol{x}_{t-1}) p(\boldsymbol{x}_{t-1}|\boldsymbol{y}_{1:t-1}) d\boldsymbol{x}_{t-1}. \qquad (23)$$

Combining $p(\boldsymbol{x}_t|\boldsymbol{y}_{1:t-1})$ with the observation $\boldsymbol{y}_t$, we have the posterior distribution $p(\boldsymbol{x}_t|\boldsymbol{y}_{1:t})$ as

$$p(\boldsymbol{x}_t|\boldsymbol{y}_{1:t}) = \frac{p(\boldsymbol{y}_t|\boldsymbol{x}_t) p(\boldsymbol{x}_t|\boldsymbol{y}_{1:t-1})}{\int p(\boldsymbol{y}_t|\boldsymbol{x}_t) p(\boldsymbol{x}_t|\boldsymbol{y}_{1:t-1}) d\boldsymbol{x}_t}. \qquad (24)$$

Applying Eqs. (23) and (24) recursively, we can obtain the conditional PDF $p(\boldsymbol{x}_t|\boldsymbol{y}_{1:t})$ for all time steps of interest. The estimate of $\boldsymbol{x}_t$ at each time step is obtained based on the conditional PDF $p(\boldsymbol{x}_t|\boldsymbol{y}_{1:t})$. Here, we calculate the mean and covariances of the PDF $p(\boldsymbol{x}_t|\boldsymbol{y}_{1:t})$ at each time step using the merging particle filter (Nakano et al., 2007) and estimate $\boldsymbol{x}_t$. The merging particle filter is an algorithm to calculate the first and second moment of a PDF from a large number of samples drawn from the PDF. In the present paper, we used 10 000 samples. A detailed explanation of this algorithm is provided in our previous papers (Nakano et al., 2007; Nakano and Higuchi, 2009).

4 Analysis

We have estimated the temporal variation of the state vector in Eq. (20) for the period from 1996 to 2003. We can then obtain the respective variations of D_{RC}, D_{MPC}, and D_{base}. Figure 2 shows the D_{st} data and the temporal variations of D_{RC}, D_{MPC}, and D_{base} for one year in 1999. As described above, the estimates for the periods during which the solar-wind data are missing for more than 6 h are excluded. The variation of D_{st} was attributed primarily to D_{RC}. However, the positive deviation of D_{st} around June can not be explained by D_{RC} because the effect of the ring current can not be positive. The effect of the magnetopause current was very small and it rather decreased than increased around June. This indicates that the positive deviation of D_{st} would not be caused by the magnetopause-current effect. The positive deviation of D_{st} is thus attributed to the increase of the non-storm component D_{base}.

Figure 3 shows D_{base} from 1996 to 2003. The variation of D_{base} is somewhat periodic; that is, D_{base} tends to be high in summer and tends to drop around spring and autumn. However, an irregular variation can also be discriminated. The amplitude and pattern of the D_{base} variation changes year by year. Note that D_{base} was unusually high around the middle of 1999 in contrast with the previous and the subsequent year. This suggests that the seasonal variation is only a part of the variation of the quiet level of D_{st} and that an irregular variation is also significant.

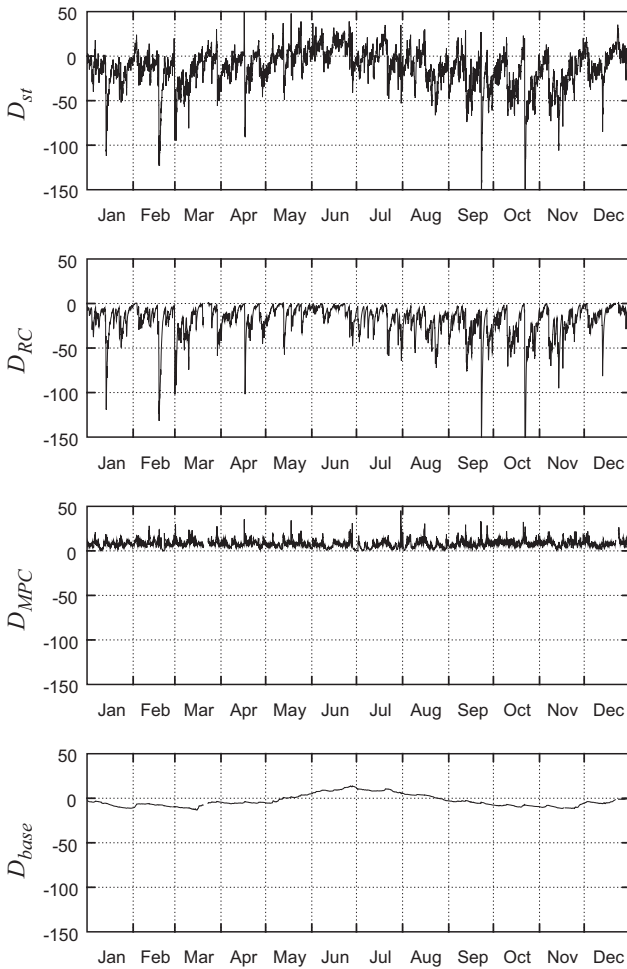In Fig. 2, the variation in D_{base} appears to be related to the long-term storm activity. Around June, when D_{base} was

Fig. 2. Variation of the D_{st} index (top panel) and the estimated variations of D_{RC} (second panel), D_{MPC} (third panel), and D_{base} (bottom panel) for one year in 1999.
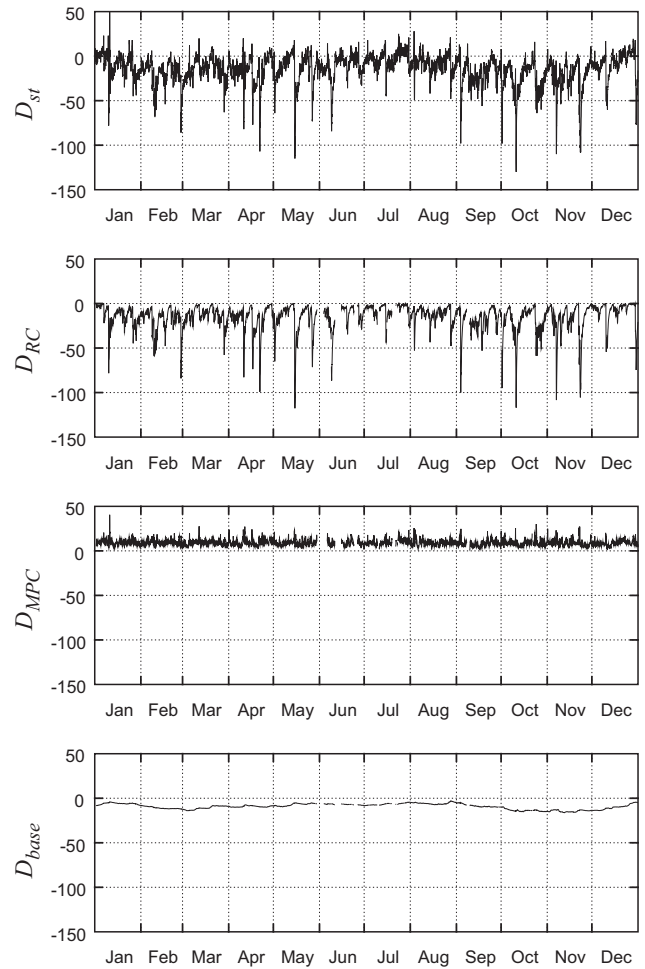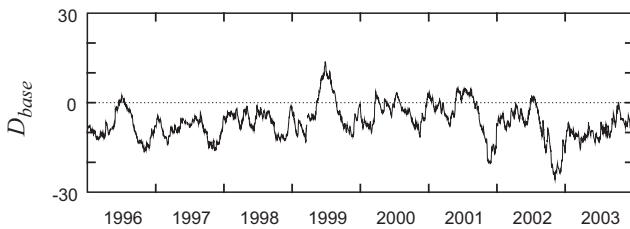

Fig. 4. Variation of the D_{st} index (top panel) and the estimated variations of D_{RC} (second panel), D_{MPC} (third panel), and D_{base} (bottom panel) for one year in 1997.

Fig. 3. Estimated variation of D_{base} from 1996 to 2003.

high, the storm activity was low, and only weak storms were observed. However, this interpretation might be hasty. Figure 4 shows the D_{st} data and the estimated D_{RC}, D_{MPC}, and D_{base} in 1997. Although storm activity was low around June, as in 1999, unlike in 1999, D_{base} remains low.

This irregular variation is likely to be controlled by a long-term variation of solar wind conditions. Figure 5 shows the 30-day moving average of the solar-wind electric field

and the solar-wind dynamic pressure. In taking the moving average, when the solar-wind magnetic field is northward, the solar-wind electric field is regarded as zero. During the northern summer of 1999, when D_{base} was high, the solar-wind dynamic pressure was extremely low and the solar-wind electric field was also low. In general, the variation of D_{base} appears to be anti-correlated with the solar-wind activity. Figure 6 compares D_{base} with the 30-day moving averages of four solar-wind parameters. All four of the parameters appear to be anti-correlated with D_{base} in terms of the 30-day moving average. In particular, the long-term variation of the solar-wind dynamic pressure exhibits a clear anti-correlation with D_{base}, as shown in Fig. 6b. (The correlation coefficient between D_{base} and the solar-wind dynamic pressure was -0.43, while the correlation coefficients with D_{base} were less than 0.3 for the other three parameters.) This suggests that the D_{st} index tends to be enhanced under the long low-pressure solar wind conditions.
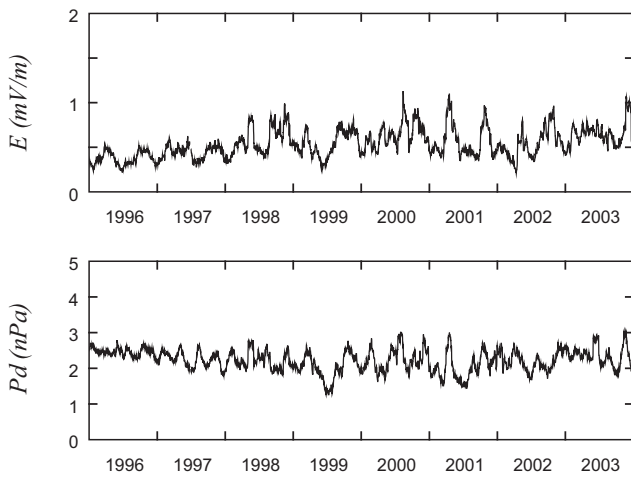
Fig. 5. Long-term variations (30-day averages) of the solar-wind electric field (top panel) and the solar-wind dynamic pressure (bottom panel) from 1996 to 2003.

The correlation between D_{base} and the solar-wind dynamic pressure becomes clearer if we use the moving geometric average of P_d instead of the moving arithmetic average of P_d. The geometric average of P_d is the exponential of the arithmetic average of $\log P_d$, and thus it places more weight on smaller P_d values and less weight on larger P_d values. Figure 7 compares between D_{base} and the 30-day moving geometric averages of the solar-wind four solar-wind parameters. The correlation coefficient is -0.52. The statistical significance of this relationship can be evaluated on the basis of the probability of obtaining the observed correlation coefficient from uncorrelated data by chance, which is called the p-value. Since the present analysis provides a variation with a time scale of about one month, we assume that the number of independent data is about 96 (12 months for each of eight years from 1996 to 2003). Under this assumption, one-tailed t-test shows that the p-value is about 3×10^{-6} %. Thus, the anti-correlation we observe can be considered to be statistically significant. In this figure, we also plotted the median for each interval of 0.2 nPa (e.g. $0.8 \le P_d < 1.0$, $1.0 \le P_d < 1.2$, ...) with a red line. The median of D_{base} decreases as P_d increases.

Before concluding that causality exists between the solar-wind dynamic pressure P_d and D_{base}, we must point out some points that could cause a spurious relationship. One of such points arises from the method of analysis. We decomposed the variation of D_{st} into three components: D_{RC}, D_{MPC}, and D_{base}. As in Eq. (11), D_{MPC} is assumed to be a function of the solar-wind dynamic pressure P_d because the short-term variation of the solar-wind dynamic pressure P_d instantaneously enhances the D_{st} index through a magnetopause current. If the coefficient b on $\sqrt{P_d}$ in Eq. (11) is overestimated, this could result in a spurious anti-correlation between D_{base} and the 30-day average of P_d because the ex-

cessive dependence of D_{MPC} on P_d could be compensated for by D_{base} in our decomposition of D_{st}. In order to exclude this spurious anti-correlation, the line of $-7.7\sqrt{P_d}$ is shown in Fig. 7. According to Eq. (11), under a given P_d value, D_{MPC} becomes at most $7.7\sqrt{P_d}$. Hence, even if the true magnetopause current effect was zero, the misestimation of D_{MPC} is at most $7.7\sqrt{P_d}$. The line of $-7.7\sqrt{P_d}$ indicates the case in which the true magnetopause current effect was zero and that the misestimation of D_{MPC} was fully compensated for by D_{base}. The spurious effect due to the misestimation of D_{MPC} is thus $-7.7\sqrt{P_d}$ at worst. Apparently, the negative effect of P_d on D_{base} is much greater than the worst case. Moreover, the positive D_{base} under the conditions of low P_d can not be explained by the misestimation of D_{MPC}. The spurious anti-correlation due to the misestimation of D_{MPC} is therefore minor if any.

Seasonal variations are another consideration. The quiet-time D_{st} exhibits seasonal dependence (Cliver et al., 2001; Mursula and Karinen, 2005), although its mechanism has not yet been clarified. On the other hand, the solar-wind conditions around Earth might exhibit seasonal dependence. For example, since the solar-wind velocity depends on heliographic latitude (e.g. Neugebauer, 1999) and the Earth's orbit is inclined from the Sun's equator, a seasonal variation of the solar-wind velocity could be observed around Earth, although a recent study suggests that the seasonal variation of the solar-wind velocity might not be significant (Svalgaard, 2011). If we assume a seasonal variation of the solar-wind conditions, a spurious relationship could be observed even if the seasonal variation of the base level of D_{st} is not caused by that of the solar-wind conditions. In order to remove the seasonal effect, we compare D_{base} and the 30-day geometric average of P_d for the four seasons in Fig. 8. Anti-correlation is observed for all four seasons. Although the correlation was relatively poor in northern autumn (August to October) and northern winter (November to January), the clear anti-correlation in northern spring (February to April) and northern summer (May to July) would be sufficient to judge that the anti-correlation is independent of the seasonal effect. Therefore, it seems reasonable to conclude that a causal relation exists between the long-term variation of solar-wind condition and D_{base}.

5 Discussion

The relationship between the solar-wind dynamic pressure P_d and the ring current intensity measured by the D_{st} index has been discussed extensively in the literature. The solar-wind density correlates with the plasma-sheet density (e.g. Terasawa et al., 1997; Borovsky et al., 1998) and numerical modeling studies have shown that high plasma-sheet density enhances the strength of the ring current (e.g. Chen et al., 1994; Jordanova et al., 1998; Kozyra et al., 1998; Ebihara and Ejiri, 2000; Nakano et al., 2008). From these studies,
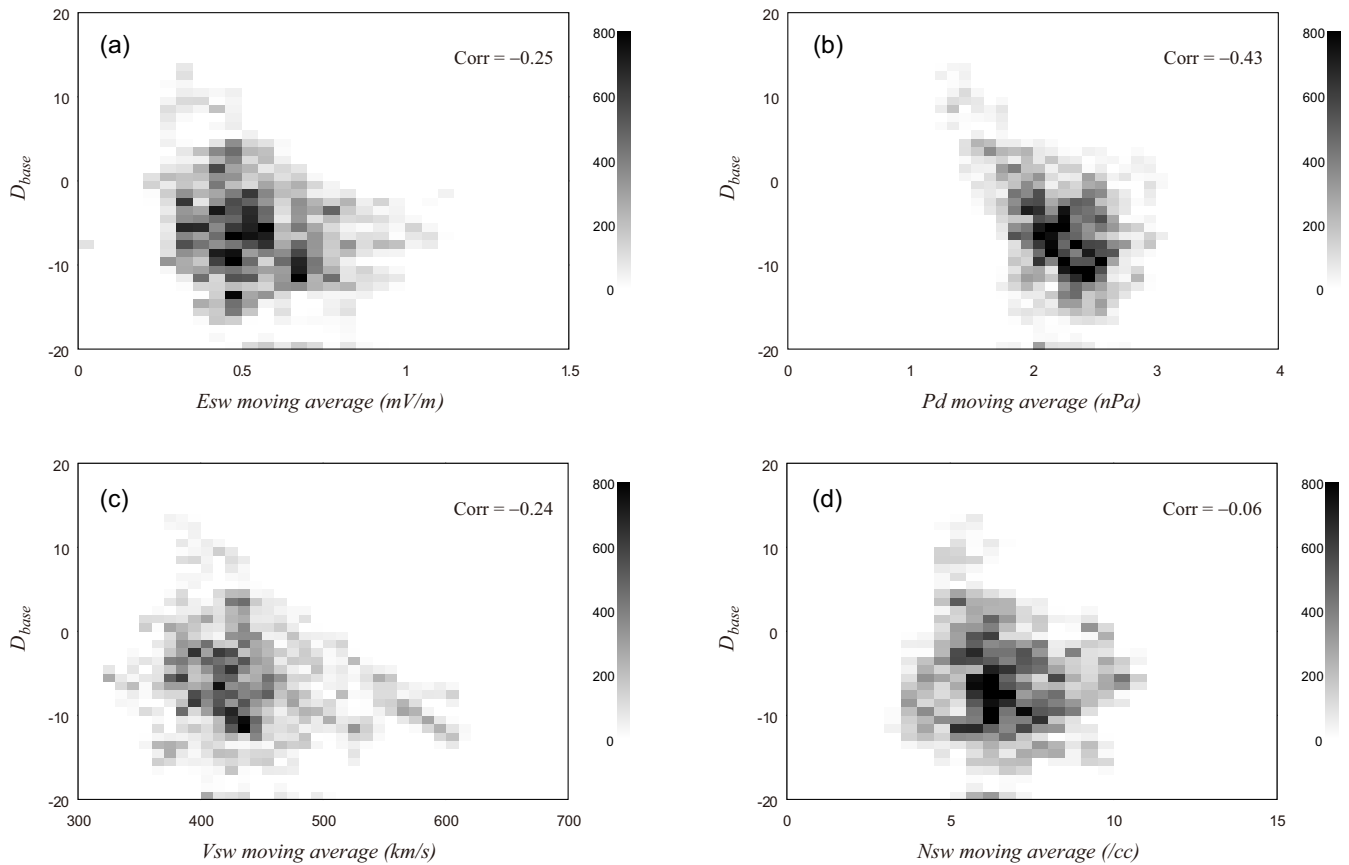
Fig. 6. Two-dimensional histograms comparing D_{base} and the 30-day moving averages of solar-wind parameters: **(a)** electric field, **(b)** solar-wind dynamic pressure, **(c)** speed, and **(d)** number density. The correlation coefficient with D_{base} was -0.25 for the solar-wind electric field, -0.43 for the solar-wind dynamic pressure, -0.24 for the solar-wind speed, and -0.06 for the solar-wind number density.
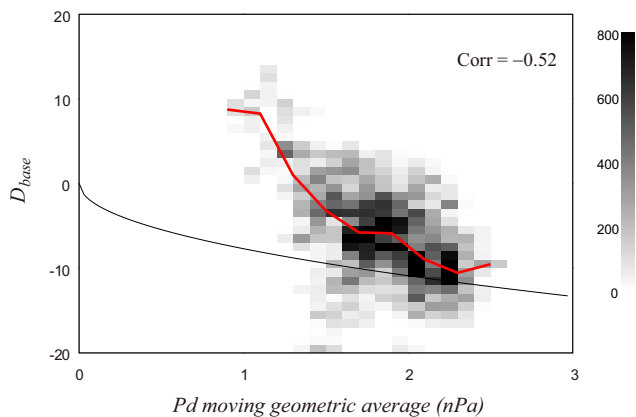

Fig. 7. Two-dimensional histograms comparing D_{base} and the 30-day moving geometric averages of solar-wind dynamic pressure. The correlation coefficient was -0.52. The red solid line indicates the median for each interval of 0.2 nPa. The black solid line indicates the line of $-7.7\sqrt{P_{\mathrm{d}}}$ (see text).

we can deduce the relationship between P_{d} and D_{st}. On the other hand, some studies have argued that the relationship between P_{d} and D_{st} is due to the dependence of transpolar potential saturation on P_{d} (Xie et al., 2008; Weigel, 2010). However, these studies have not provided an explanation for the anti-correlation between the long-term variation of P_{d} and the non-storm component of D_{st} demonstrated in the present study.

Burton et al. (1975) assumed that D_{st}^{*} (or D_{RC}) cannot decay further after recovering to the quiet level, 0, as described in Eq. (2). According to this assumption and Eq. (1), if the magnetopause current is in the normal level to satisfy

$$D_{\mathrm{MPC}}(=b\sqrt{P_{\mathrm{d}}})=c, \tag{25}$$

then the D_{st} index cannot be above zero. However, zero D_{st} does not indicate that the ring current and tail current become zero. Even if D_{st} is zero, weak ring and tail currents would continue to exist (e.g. Sugiura, 1973; Grafe, 1999; Tsyganenko et al., 1999). Therefore, we can speculate that if the ring and tail currents are unusually depleted, D_{st} can be increased to be greater than zero without enhancement of the magnetopause current. The enhancement of D_{base} could
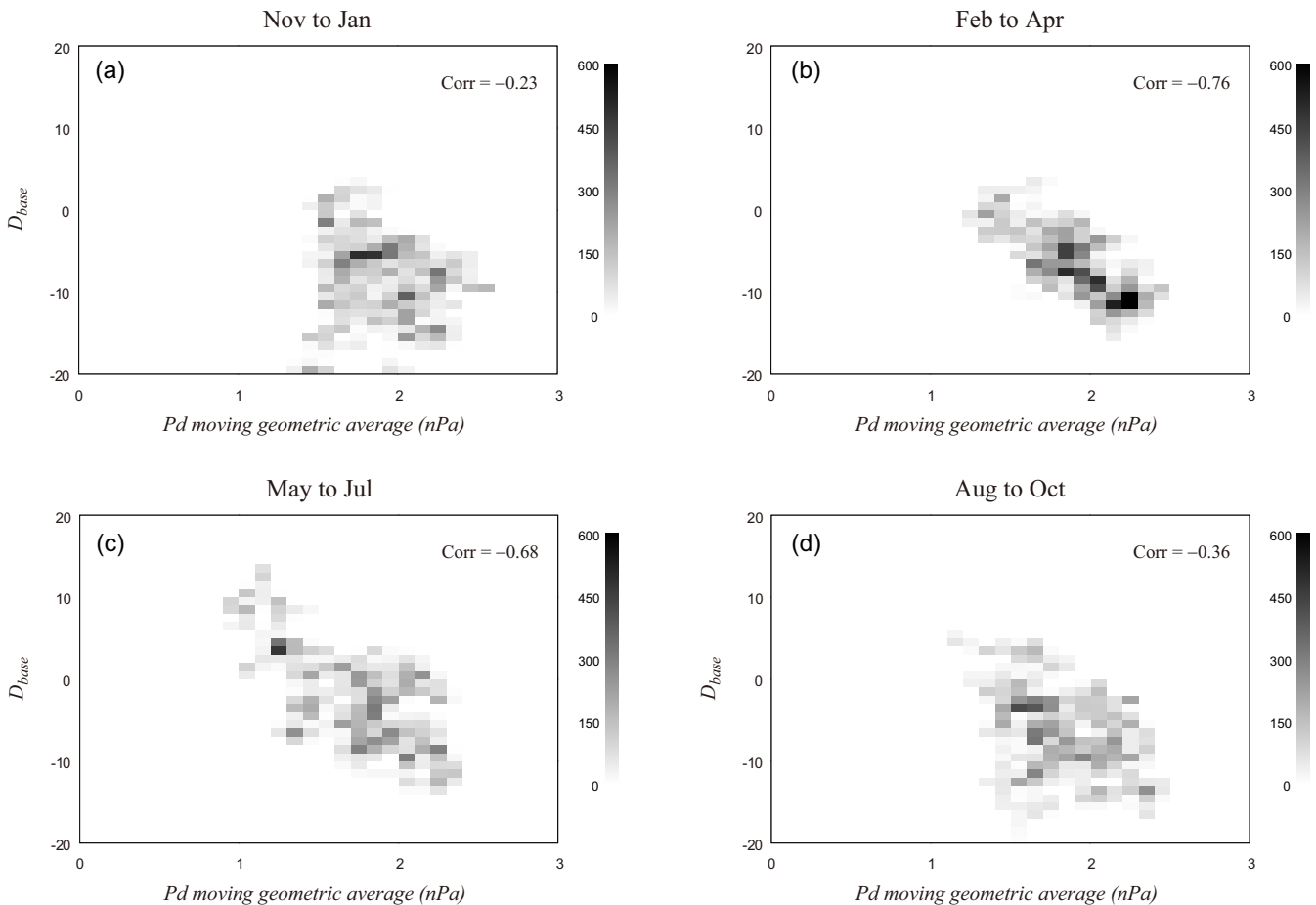
Fig. 8. Two-dimensional histograms to compare between D_{base} and the 30-day moving geometric averages of solar-wind dynamic pressure for four seasons: **(a)** November to January, **(b)** February to April, **(c)** May to July, and **(d)** August to October. The correlation coefficient between D_{base} and solar-wind dynamic pressure was -0.23, -0.76, -0.68, and -0.36, respectively.

reflect this increase in D_{st} due to the unusual depletion of the ring and tail currents. It has been observationally established that the solar-wind dynamic pressure correlates with the thermal pressure in the plasma sheet (Borovsky et al., 1998) even in the near-Earth region (Tsyganenko and Mukai, 2003; Denton and Borovsky, 2008). Then, extremely low solar-wind dynamic pressure would cause unusual plasma energy depletion in the magnetosphere. This should result in an increase in D_{base} because the value of D_{st} is related to the total thermal energy in the magnetosphere (Dessler and Parker, 1959; Sckopke, 1966; Siscoe, 1970; Siscoe and Petschek, 1997). While the plasma-sheet plasma is denser under northward interplanetary magnetic field (IMF) conditions, it is hotter under southward IMF conditions (Terasawa et al., 1997; Nagata et al., 2007, 2008). After all, the dependence of the plasma-sheet thermal pressure on IMF is low (Tsyganenko and Mukai, 2003). Accordingly, the variation of the plasma-sheet thermal pressure would be observed as a non-storm phenomenon without being closely related to IMF.

It would be informative to estimate the time scale of the D_{base} variation in response to the solar-wind activity changes in order to clarify the mechanism causing the anti-correlation between D_{base} and the solar-wind dynamic pressure. However, our method does not allow the time scale to be inferred. We assumed small variability of D_{base} in order to ensure that the estimate of D_{base} is not influenced by short-term variations due to D_{RC} and D_{MPC}. Although we compared the estimated D_{base} with the 30-day averages of solar-wind parameters, this does not mean that the time scale of the D_{base} variation is 30 days. In fact, the time scale of the D_{base} variation could be much less than 30 days. Hence, it is difficult to determine the non-storm short-term variation using this method and to determine the time scale of the non-storm variation. However, it might be helpful to consider the fact that D_{base} shows better correlation with the moving geometric average of the solar-wind dynamic pressure than with its moving arithmetic average. Since a geometric average tends to place less weight on larger values, the improvement obtained using the geometric average might indicate that the

short-term strong enhancement of P_d has only a minor effect on the D_{base} variation.

The reason for the different correlation among the different seasons in Fig. 8 remains an open question. (The correlation coefficient between D_{base} and 30-day averages of P_d was -0.23 for November to January, -0.76 for February to April, -0.68 for May to July, and -0.36 for August and October.) This may have a physical meaning, but it may be caused by statistical dispersion because we could use only the quarter of the data for each season. In order to evaluate the statistical dispersion, we performed a rough bootstrap test (Efron, 1981). Here, we used monthly values of P_d and D_{base} because the present analysis provides a variation with a time scale of about one month. The data for each season are for 24 months, which are a quarter of 96 months in eight years from 1996 to 2003. We thus evaluated the statistical dispersion of the correlation coefficient calculated from arbitrary data for 24 months of the 96 months. The bootstrap test suggests that the correlation coefficient can be above -0.36 with a probability of 15 % and above -0.23 with a probability of 7 %. Thus we cannot necessarily exclude the possibility of the statistical dispersion. In order to assess whether the difference in correlation has a physical meaning, further analysis with a larger data set (for a longer period) is required.

6   Summary

We decomposed the variation of D_{st} into the three components: the effect of the ring and tail currents D_{RC}, the effect of the magnetopause current D_{MPC}, and the non-storm component D_{base}. We then examined the temporal evolution of D_{base} from 1996 to 2003. The results indicate that D_{base} was unusually high around June 1999, when the solar-wind activity was low. In general, D_{base} is likely to be anti-correlated with long-term solar-wind activity, especially with the long-term variation of the dynamic pressure. We interpret this result as indicating that the irregular variation of D_{base} is caused primarily by the non-storm tail current variation due to the change of the plasma-sheet thermal pressure. The anti-correlation between the long-term dynamic pressure and D_{base} is observed even if the seasonal dependence is removed. This means that this anti-correlation exists independently of the seasonal effects.

References

Borovsky, J. E., Thomsen, M. F., and Elphic, R. C.: The driving of the plasma sheet by the solar wind, J. Geophys. Res., 103, 17617–17639, 1998.

Burton, R. K., McPherron, R. L., and Russell, C. T.: An empirical relationship between interplanetary conditions and *Dst*, J. Geophys. Res., 80, 4204–4214, 1975.

Chen, M. W., Lyons, L. R., and Schulz, M.: Simulations of phase space distributions of storm time proton ring current, J. Geophys. Res., 99, 5745–5759, 1994.

Cliver, E. W., Kamide, Y., and Ling, A. G.: Mountain and valleys: Semiannual variation of geomagnetic activity, J. Geophys. Res., 105, 2413–2424, 2000.

Cliver, E. W., Kamide, Y., Ling, A. G., and Yokoyama, N.: Semi-annual variation of the geomagnetic *Dst* index: Evidence for a dominant nonstorm component, J. Geophys. Res., 106, 21297–21304, 2001.

Denton, M. H. and Borovsky, J. E.: Superposed epoch analysis of high-speed-stream effects at geosynchronous orbit: Hot plasma, cold plasma, and the solar wind, J. Geophys. Res., 113, A07216, doi:10.1029/2007JA012998, 2008.

Dessler, A. J. and Parker, E. N.: Hydromagnetic theory of geomagnetic storms, J. Geophys. Res., 64, 2239–2252, 1959.

Ebihara, Y. and Ejiri, M.: Simulation study on fundamental properties of the storm-time ring current, J. Geophys. Res., 105, 15843–15859, 2000.

Efron, B.: Nonparametric estimates of standard error: The jack-knife, the bootstrap and other methods, Biometrika, 68, 589–599, 1981.

Grafe, A.: Are our ideas about *Dst* correct?, Ann. Geophys., 17, 1–10, doi:10.1007/s00585-999-0001-0, 1999.

Jordanova, V. K., Farrugia, C. J., Janoo, L., Quinn, J. M., Torbert, R. B., Ogilvie, K. W., Lepping, R. P., Steinberg, J. T., McComas, D. J., and Belian, R. D.: October 1995 magnetic cloud and accompanying storm activity: Ring current evolution, J. Geophys. Res., 103, 79–92, 1998.

Kitagawa, G.: Monte Carlo filter and smoother for non-Gaussian nonlinear state space models, J. Comp. Graph. Statist., 5, 1–25, 1996.

Kozyra, J. U., Jordanova, V. K., Borovsky, J. E., Thomsen, M. F., Knipp, D. J., Evans, D. S., McComas, D. J., and Cayton, T. E.: Effects of a high-density plasma sheet on ring current development during the November 2–6, 1993, magnetic storm, J. Geophys. Res., 103, 26285–26305, 1998.

Mayaud, P. N.: The annual and daily variations of the Dst index, Geophys. J. R. Astr. Soc., 55, 193–201, 1978.

Mursula, K. and Karinen, A.: Explaining and correcting the excessive semiannual variation in the *Dst* index, Geophys. Res. Lett., 32, L14107, doi:10.1029/2005GL023132, 2005.

Nagata, D., Machida, S., Ohtani, S., Saito, Y., and Mukai, T.: Solar wind control of plasma number density in the near-Earth plasma sheet, J. Geophys. Res., 112, A09204, doi:10.1029/2007JA012284, 2007.

Nagata, D., Machida, S., Ohtani, S., Saito, Y., and Mukai, T.: Solar wind control of plasma number density in the near-Earth plasma sheet: three-dimensional structure, Ann. Geophys., 26, 4031–4049, doi:10.5194/angeo-26-4031-2008, 2008.

Nakano, S. and Higuchi, T.: Estimation of a long-term variation of a magnetic-storm index using the merging particle filter, IEICE

Trans. Inf. and Syst., E92-D, 1382–1387, 2009.

Nakano, S., Ueno, G., and Higuchi, T.: Merging particle filter for sequential data assimilation, Nonlin. Processes Geophys., 14, 395–408, doi:10.5194/npg-14-395-2007, 2007.

Nakano, S., Ueno, G., Ebihara, Y., Fok, M.-C., Ohtani, S., Brandt, P. C., Mitchell, D. G., Keika, K., and Higuchi, T.: A method for estimating the ring current structure and the electric potential distribution using ENA data assimilation, J. Geophys. Res., 113, A05208, doi:10.1029/2006JA011853, 2008.

Neugebauer, M.: The three-dimensional solar wind at solar activity minimum, Rev. Geophys., 37, 107–126, 1999.

O'Brien, T. P. and McPherron, R. L.: An empirical phase space analysis of ring current dynamics: Solar wind control of injection and decay, J. Geophys. Res., 105, 7707–7719, 2000.

O'Brien, T. P. and McPherron, R. L.: Seasonal and diurnal variation of Dst dynamics, J. Geophys. Res., 107, 1341, doi:10.1029/2002JA009435, 2002.

Sckopke, N.: A general relation between the energy of trapped particles and the disturbance field near the Earth, J. Geophys. Res., 71, 3125–3130, 1966.

Siscoe, G. L.: The virial theorem applied to magnetospheric dynamics, J. Geophys. Res., 75, 5340–5350, 1970.

Siscoe, G. L. and Petschek, H. E.: On storm weakening during substorm expansion phase, Ann. Geophys., 15, 211–216, doi:10.1007/s00585-997-0211-2, 1997.

Sugiura, M.: Quiet time magnetospheric field depression at 2.3–3.6 R_E, J. Geophys. Res., 78, 3182–3185, 1973.

Svalgaard, L.: Geomagnetic semiannual variation is not overestimated and is not an artifact of systematic solar hemispheric asymmetry, Geophys. Res. Lett., 38, L16107, doi:10.1029/2011GL048616, 2011.

Terasawa, T., Fujimoto, M., Mukai, T., Shinohara, I., Saito, Y., Yamamoto, T., Machida, S., Kokubun, S., Lazarus, A. J., Steinberg, J. T., and Lepping, R. P.: Solar wind control of density and temperature in the near-Earth plasma sheet: WIND/GEOTAIL collaboration, Geophys. Res. Lett., 24, 935–938, 1997.

Tsyganenko, N. A. and Mukai, T.: Tail plasma sheet models derived from Geotail particle data, J. Geophys. Res., 108, 1136, doi:10.1029/2002JA009707, 2003.

Tsyganenko, N. A., Le, G., Russell, C. T., and Iyemori, T.: A study of the inner magnetosphere based on data of Polar, J. Geophys. Res., 104, 10275–10283, 1999.

Wang, C. B., Chao, J. K., and Lin, C.-H.: Influence of the solar wind dynamic pressure on the decay and injection of the ring current, J. Geophys. Res., 108, 1341, doi:10.1029/2003JA009851, 2003.

Weigel, R. S.: Solar wind density influence on geomagnetic storm intensity, J. Geophys. Res., 115, A09201, doi:10.1029/2009JA015062, 2010.

Xie, H., Gopalswamy, N., St. Cyr, O. C., and Yashiro, S.: Effects of solar wind dynamic pressure and preconditioning on large geomagnetic storms, Geophys. Res. Lett., 35, L06S08, doi:10.1029/2007GL032298, 2008.